Electronic Spectroscopy of C_2 in Solid Rare Gas Matrixes

Steven L. Fiedler, Kari J. Vaskonen, Jussi M. Eloranta, and Henrik M. Kunttu*

Nanoscience Center, Department of Chemistry, P.O. Box 35, 40014 University of Jyväskylä, Finland

Received: January 7, 2005; In Final Form: March 29, 2005

Electronic spectroscopy of the C_2 molecule is investigated in Ar, Kr, and Xe matrixes in the 150−500 nm range. In the Ar matrix, the D ($^1\Sigma_u^+$) ← ($^1\Sigma_g^+$) Mulliken band near 240 nm is the sole absorption in the UV range, whereas in the Kr matrix additional bands in the 188−209 nm range are assigned to the $Kr_n^+C_2^-$ ← Kr_nC_2 charge-transfer absorptions. Because of the formation of a bound C_2Xe species, the spectral observations in the Xe matrix differ dramatically from the lighter rare gases: the Mulliken band is absent and new bands appear near 300 and 423 nm. The latter is assigned to the forbidden B′($^1\Sigma_g^+$) ← X ($^1\Sigma_g^+$) transition, but the origin of the former remains unclear. The spectral assignments are aided by electronic structure calculations at the MCSCF, CCSD(T), and BCCD(T) levels of theory and correlation consistent basis sets. A significant presence of multireference character of the C_2Xe system was noted and a linear ground-state structure is predicted. The computational results contradict previous density functional studies on the same system.

Introduction

It has been known for quite some time that solid rare gas matrixes, besides providing an inert environment for isolating chemical species of interest, are rather ideally suited as model systems for studies on guest−host interactions and their implication in elementary chemical events. A vast body of recent work on this subject was recently reviewed by Apkarian and Schwentner.[1] In general, the closed-shell electronic structure of rare gas atoms makes these systems relatively weakly interacting as indicated by only small spectral shifts in the guests' spectra. This is particularly true for the lighter rare gases Ne and Ar, in which vibrational frequencies are typically shifted by few wavenumbers from their gas-phase values.[2] However, in certain conditions, rare gases turn from weakly interacting to strongly interacting systems and in extreme cases, chemical bonds involving rare gas atoms are formed. The extensive series of investigations by Räsänen et al. starting from the mid 1990s has shown that rare gases have, in fact, a more diverse chemistry than originally expected.[3] Among the newly discovered molecules is the C_2Xe molecule, which is the smallest of the nonhydride member of the family of rare gas compounds C_nXe, ($n = 2, 3, ...$).[4−6]

Intermolecular guest−host charge-transfer (CT) transitions provide a versatile tool to study the many-body nature of guest−host interactions in condensed matter. These transitions have large transition dipoles and the spectra can be well understood in terms of localized and delocalized ion-hole states. We have recently reported a detailed analysis on such systems, CN doped solid Kr and Xe, on the basis of the diatomics-in-ionic-systems (DIIS) formalism.[7] It was shown that the charge-transfer absorption of CN closely resembles observations in Cl doped Kr and Xe, and the difference can be almost entirely ascribed to the electron affinity of the acceptor. This observation served as our motivation to extend our studies to another very similar electron acceptor, the C_2 molecule, which has electron affinity similar to Cl atom and CN radical. In a previous report, we presented DIIS predictions of the charge-transfer absorptions of C_2 doped Kr clusters of various size.[8] In this paper, we show the UV absorption spectra of extensively photolyzed acetylene doped Ar, Kr, and Xe matrixes down to 150 nm. It will be shown that charge-transfer bands can be confidently assigned only in Kr matrix.

To aid interpretation of spectral observations of the C_2 doped Xe matrix, ab initio calculations were carried out for the ground and excited electronic states of C_2−Xe pair. While knowledge of relevant potential energy surfaces (PES) often provide a better spectroscopic understanding, the large number of electrons associated with the Xe atom places a high demand on computational resources. To the authors' knowledge, studies to date have only calculated the C_2Xe ground-state interaction potential, and no calculations on the excited electronic states have been reported.[5,9] While spectroscopy is sensitive to a many-bodied PES, many important questions can be addressed through knowledge of the dopant/host pair potentials only. In this study, we employed the coupled cluster with single, double, and perturbative triple excitations CCSD(T), multiconfiguration self-consistent field (MCSCF), and the Brueckner coupled-cluster method BCCD(T) to this end.

Experimental Section

Pure acetylene was synthesized in a manner similar to that previously outlined by Milligan et al.[10] Purity of the product was verified by measuring the IR spectrum of the product isolated in the rare gas matrix. The following matrix gases were used: Ar (99.9999%, AGA), Kr (Scientific Grade, AGA), Xe (99.997%, AGA).

The gas samples were prepared in an all-glass vacuum manifold, evacuated to better than 5×10^{-5} mbar with a diffusion pump. The pressure of acetylene added to the mixing chamber ranged from 0.22 mbar to 1 mbar and it was mixed with a rare gas at pressures between 400 and 1000 mbar yielding typical guest/host ratios 1:1000−1:10000. The gas mixture was transferred to a 1-L Pyrex sample bulb and then deposited on MgF_2 substrate window, which was cooled to 15 K, 25 K, and 30−50 K for Ar, Kr, and Xe matrixes, respectively. A closed

* Author to whom correspondence should be addressed. E-mail: Henrik.Kunttu@jyu.fi.

10.1021/jp0500992 CCC: $30.25
Published on Web 04/28/2005

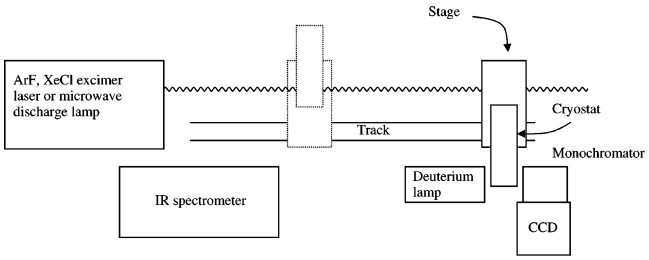

Figure 1. Experimental setup for measuring both IR and UV absorptions from the same sample is shown.

TABLE 1: Summary of Photofragment IR Absorptions (1100−3500 cm^{-1}) Observed in the Photolysis of Acetylene in Rare Gas Matrixes[a]

fragment	absorptions
C_2H_2	$\nu_4 + \nu_5$: 1328 and 1340 gas,[20] 1335 Ar,[21] **(1327)** ~1330 Kr,[22] **1317** Xe[18]
	$\nu_2 + \nu_4 + \nu_5$: 3282 gas,[23] 3289 Ar,[24] **3280** Kr, **3267** Xe
	ν_3: 3295 gas,[23] 3303 Ar,[24] **3293** Kr, **3280** Xe[18]
$(C_2H_2)_2$	ν_3: 3272 gas,[25] **3249** and **(3252)** 3251 Xe[4]
C_2H	ν_3: 1841 gas,[26] 1835 Ne,[27,28] **1846** Ar,[28] **1842** Kr,[22] 1852 Xe[18]
$HRgC_2H$	**1242**, **1250**, **(1256)** 1257, **3290** Kr,[22] 1486, 3273 Xe[19]

[a] Values from this work are listed in bold, and values that deviate from literature values are indicated in parenthesis.

cycle cryostat (Displex DE-202A, APD Cryogenics, Inc.) was used for cooling. Deposition rates of 0.06−0.12 mmol/min were used to grow samples, and the total amount of deposited gas varied between 3.5 and 6.0 mmol. The vacuum shroud was equipped with MgF_2 windows, which limited our observation window in the infrared range to 1200 cm^{-1} but provided transparency deep in the vacuum ultraviolet (VUV) range. Matrix isolated acetylene was photolyzed primarily by an atomic Kr resonance lamp, which was driven by microwave discharge source (Sairem). Additionally, a 308 nm (XeCl) excimer laser (Estonian Academy of Sciences, ELI-94) was used for indirect photolysis of acetylene in the Xe matrix by two-photon generation of the Xe excitons and subsequent energy transfer.[4]

The infrared measurements were made using an FTIR spectrometer (Nicolet Magna IR 760), equipped with a HgCdTe detector and a KBr beam splitter. Absorption measurements in the visible and UV range employed a spectrometer consisting of a 30 W deuterium lamp source equipped with MgF_2 window, 125-mm spectrograph (Oriel Instruments, MS125), and an ICCD camera (Andor Technologies). The optical path of the VUV light was continuously flushed with nitrogen gas to avoid air absorption. To be able to record both IR and UV absorption spectra after a given amount of radiation dose reliably, the cryostat was mounted on a stage and a track as shown in Figure 1. This enabled facile transfer of the cryostat from the FTIR to the UV spectrometer and allowed for correlation of the spectra in these two regions.

Computational Methods and Parameters. The computational methods employed were the Hartree−Fock (HF), coupled clusters with single, double, and perturbative triple excitations CCSD(T), multiconfiguration self-consistent field (MCSCF), and the Brueckner coupled cluster method BCCD(T).[11,12] The carbon basis consisted of the Dunning correlation consistent polarized valence X-zeta basis (cc-pVXZ) with X specified as doubles (D), through 5, and augmented cc-pVXZ (aug-cc-pVXZ).[13] The Xe basis consisted of the correlation consistent small-core (1s−3d) relativistic psudopotential cc-pVXZ-PP or the augmented extension, aug-cc-pVXZ-PP.[14] In all calculations, the core orbitals were set as the C 1s and Xe 4s, 4p, and 4d. The active space in the MCSCF calculations included the remainder of the valence states of C_2 and the 5s and 5p orbitals of Xe. The asymptotic limits of the excited valence states calculated by the MCSCF method were adjusted to match the experimental values.[15] Standard basis set superposition error (BSSE) correction was carried out for HF, CCSD(T), and BCCD(T) calculations by the counterpoise method of Boys and Bernardi.[16] This correction is not possible in practice for MCSCF calculations; however, in the limit of a complete basis set, the BSSE should approach zero. The reported calculations all employed spherical harmonics and were carried out using MOLPRO 2002.6 suite of programs.[17]

Experimental Results

Upon UV photolysis, the progress of dissociation of C_2H_2 was monitored via attenuation of the $\nu_2 + \nu_4 + \nu_5$ and ν_3 IR absorption bands. Dilute C_2H_2 concentrations were used to avoid aggregation of acetylene during sample deposition. The IR frequencies of plausible fragments are summarized in Table 1, including those observed in this study: C_2H/Ar, C_2H/Kr, $HKrC_2H$, $(C_2H_2)_2$/Xe, and C_2Xe. The absence of the C_2H/Xe absorption[18,19] reported at 1852 cm^{-1} is most probably attributed to the dilute precursor concentration (1:2700) as well as the possibility that our radiation sources, discussed above, immediately dissociated the C_2H intermediate.

In the UV region, the C_2 valence D ($^1\Sigma_u^+$) ← X ($^1\Sigma_g^+$) Mulliken band was present in Ar at 238 nm matching the literature value and in Kr at 248 nm (Figure 2, 3).[10] As expected, this strong absorption band was absent in the Xe matrix (Figure 4).[4] In the Kr matrix, previously unidentified absorptions with

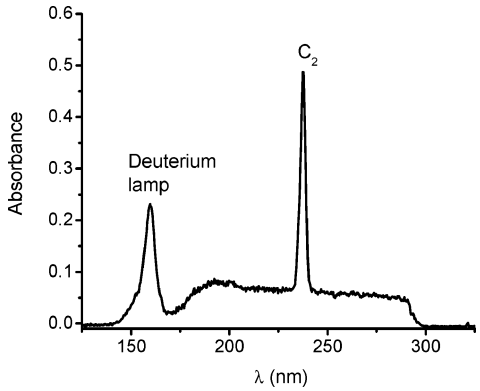

Figure 2. UV absorption spectrum of photolyzed C_2H_2/Ar sample (M/R 1:1000). Photolysis was carried out using Kr resonance lamp.

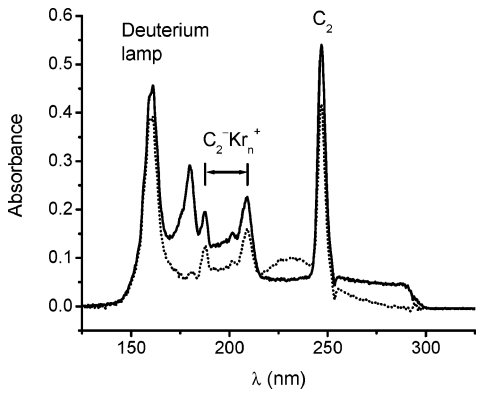

Figure 3. UV absorption spectrum of photolyzed C_2H_2/Kr sample (M/R 1:1000) before (solid) and after (dotted) annealing. Photolysis was carried out using Kr resonance lamp.

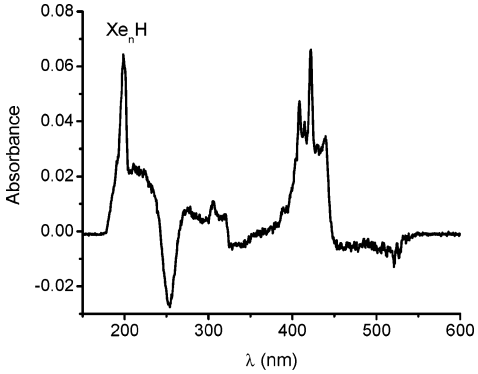

Figure 4. UV absorption spectrum of a photolyzed C_2H_2/Xe sample (M/R 1:8000). The photolysis was varied out using 308 nm excimer laser. Negative absorption at ~250 nm originates partly from acetylene absorption depletion and partly from HXe_2 exciplex emission.[29,30]

maxima at 180, 188, and 209 nm were observed as shown in Figure 3. It was found by annealing that the 180 nm band could be predominately attributed to a thermally bleachable component and therefore belonged to a different absorber than the thermally stable 188 and 209 nm bands. In the Xe matrix, unassigned bands centered near 300 and 423 nm were observed, similarly as reported by Maier and Bondybey and co-workers.[4,5] Xe$_n$H bands were also observed at ~199 nm as previously reported.[31] Electronic absorptions of atomic carbon ($^3D^0 \leftarrow {}^3P$, and $^3P^0 \leftarrow {}^3P$ lines) and the Kr caged hydrogen atom, Kr$_n$H, could not be given with confidence because of the overlap with the characteristic deuterium lamp background near 160 nm.

Computational Results

A set of calculations designed to elucidate the experimental observations first required determination of the minimum energy structure of the C_2Xe molecule in its ground state. As the PES is a multidimensional hypersurface dependent on the C−C separation (r_{CC}), C_2−Xe separation (r_{CC-Xe}), and the orientation of Xe with respect to the C_2 molecular axis (Θ_{CC-Xe}), a search for the potential energy minimum involves variation over all of these independent variables. To limit the search over the parameter space, we fixed the r_{CC} distance to that calculated for the C_2 diatomic, 1.25 Å, and only varied r_{CC-Xe}. Justification for this approximation exists, as although the charge-transfer state $C_2^-Xe^+$ is expected to mix with the ground state, the equilibration separation distance (r_e) for C_2 and C_2^- is quite close (1.246 Å vs 1.272 Å).[19]

We found notable differences in the C_2Xe pair potentials as calculated by single and multireference methods. Artificially strong binding and short intermolecular separation were predicted for the linear geometry by the HF method ($r_e = 2.6$ Å, $\Delta E = -1.1$ eV) and in the nonlinear geometries by the CCSD(T) method (Figure 5). Note $r = 0$ corresponds to the C_2 center of mass. For these nonlinear geometries, the T_1 norm, an indicator of the degree of multireference character in coupled cluster calculations, greatly exceeded the typically accepted limit of 0.02 for CCSD theory.[32] On the other hand, the BCCD(T) method, thought to be more adept at accounting for multireference character, yielded linear minimum energy structures for all values of r (Figure 5).[33] For linear geometries, the T_1 norm of the CCSD(T) calculations fell within reasonable limits ranging from 0.03 to 0.06 and is only slightly higher than the limit. Correspondingly, the resultant potential energy curve ($r_e = 3.2$ Å, $\Delta E = -87$ meV) approached that produced by BCCD(T) method ($r_e = 3.4$ Å, $\Delta E = -47$ meV).

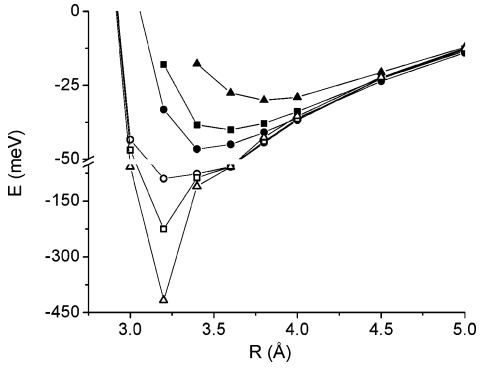

Figure 5. Pair potentials of the C_2Xe system at varying angles of the Xe with respect to the C_2 molecular axis. CCSD(T)/avqz,avqz-PP: △ 170°, □ 175°, ○ 180°; BCCD(T)/avtz,avtz-PP: ● 180°, ■ 170°, ▲ 160°. Solid lines are guides to the eye.

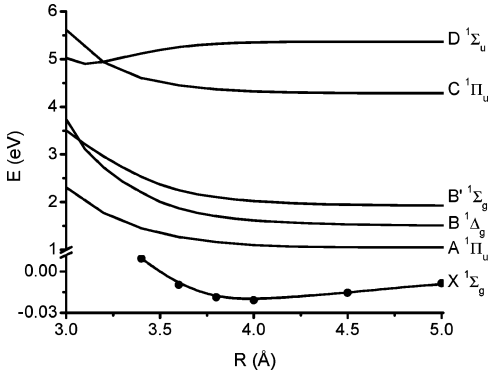

Figure 6. Calculated pair potentials of the C_2Kr system with an avqz/avqz-PP basis. The ground potential (●) was calculated by CCSD(T), upper potentials were calculated by MCSCF. Lines indicate spine fits.

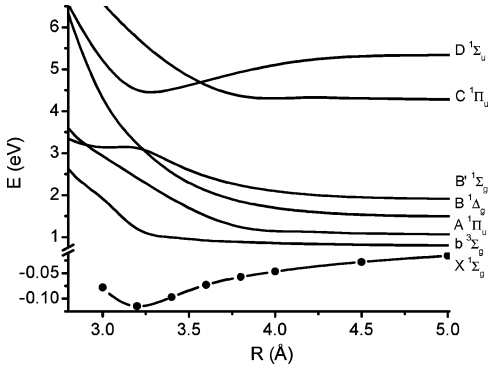

Figure 7. Equivalent potentials of Figure 6 for the C_2Xe system.

The excited states of C_2Xe were obtained only at the MCSCF level because of the high computational cost of MRCI with a large active space and the related convergence problems. Consequentially, the excited-state potentials for C_2Kr and C_2-Xe shown in Figure 6 and Figure 7, respectively, contain only static electron correlation contributions. The electronic transition dipole moments of the C_2-rare gas complex obtained from the MCSCF calculations show that the D ← X (Mulliken) transition (Figure 8) gains intensity when going from the Kr to Xe host. In addition, the B′ ← X transition (not shown) becomes strongly allowed at distances corresponding to the ground-state C_2Xe potential energy minimum because of breakdown of the u/g symmetry.

Discussion

Charge-Transfer States. The 188−209 nm set of bands in Kr matrix (Figure 3) bears close resemblance to the CN/Kr CT

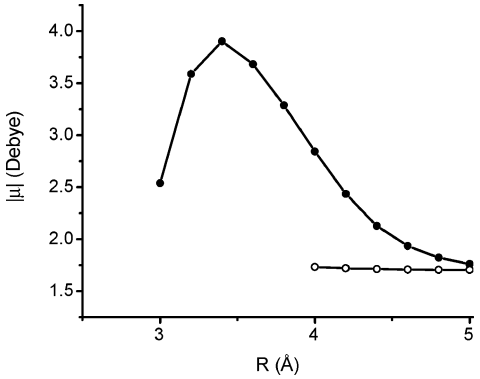

Figure 8. Absolute values for the C_2Kr (○) and C_2Xe (●) D ← X transition dipoles as a function of r_{CC-Xe}. Values were obtained by the MCSCF method with the avqz/avqz-PP basis.

bands measured and analyzed previously. The splitting of the band maxima corresponds energetically to 0.67 eV, which is close to the value 0.69 eV observed in the CN/Kr case. This splitting has been attributed to the spin−orbit constant of Kr^+ and should be independent of the dopant. As the energetics of the CT states directly correlate with the electron affinity of the guest species, the band origin should shift accordingly. For CN and C_2, the respective electron affinities of 3.86 and 3.27 eV also correlate directly with the band origins of the charge-transfer absorptions.[34] The extracted energy difference from the experimental spectra is 0.63 eV, which is close to the theoretically predicted value of 0.59 eV. Furthermore, the observed band structure compares well with our previous theoretical predictions.[8] On the basis of these arguments, we assign the 188−209 nm bands to $Kr_n^+C_2^-$ ← Kr_nC_2 CT absorptions.

As the energy of the CT states is dictated by the ionization potential of the rare gas host, the absorption band origins should shift accordingly. This would predict origins for the CT bands as Ar (161 nm), Kr (209 nm), and Xe (306 nm).[7] For the case of Ar, the presence of the strong deuterium lamp background in the 155−165 nm region could mask the CT absorptions and they could not be seen (Figure 2). In the case of Xe, shown both in this study (Figure 4) and that of Maier,[4] the absorptions located near 300 nm could belong to the CT states. However, the 300 nm region has a slightly different structure than the C_2Kr band. Measurement of the excitation spectrum of both Ar and Xe host matrixes could yield additional insight to the presence of the CT bands.

XeC_2 Ground State. An important outcome of the C_2Xe ground-state calculations is that the equilibrium geometry is linear with the BCCD(T) method. Although both CCSD(T) and BCCD(T) are based on single reference wave functions, it has been thought that the BCCD(T) could partially account for static electron correlation.[33] The significant deviation of the T_1 norm indicator from the normal range in the nonlinear CCSD(T) calculations also suggested the presence of multireference character. To understand the origin of such behavior, we have also calculated the ground-state potential energy curve by the MCSCF method. The necessity for static correlation can be explained by significant mixing of the C_2 valence σ_u*2s and $\sigma_g 2p_0$ configurations resulting in occupational weights of 1.6 and 0.4, respectively. The effect of this mixing is emphasized at the short separation distances. On the basis of the above considerations, we consider that C_2Xe exists as a linear molecule. This differs from the density functional theory (DFT) predictions reported recently.[5] As DFT is also a single reference based method, it would likely face similar difficulties in accounting for static correlation as the HF and CCSD(T) methods discussed above.

The linear C_2Xe values calculated in this study by BCCD-(T)/avtz (r_e = 3.4 Å, ΔE = −47 meV) match well with the BCCD(T)/d-avqz calculations by Breidung and Thiel (3.3 Å, −52 meV).[9] These values are very different to those reported for the linear C_2Ar (4 Å and −14 meV) and C_2Kr (4 Å and −18 meV) complexes.[8,35] Indeed, we propose this difference is the reason for unusual spectroscopy of C_2 in solid Xe. If the trapping cavity size in Xe lattice is larger than the r_e of C_2Xe, the C_2 dopant would be expected to be asymmetrically centered within the cavity. This asymmetry would make the C−C stretch mode allowed and introduce a red shift in the IR spectrum. These effects are consistent with the experimental observations.[4,5] On the basis of this consideration and the diminished binding present in the nonlinear potentials, it is likely that C_2 is essentially bound only to one Xe atom in the matrix.

Excited Electronic States of C_2 in Xe. Although the excited-state potentials obtained by the MCSCF method are coarse in nature because of lack of inclusion of dynamic correlation and counterpoise correction, they do provide a basis for a qualitative discussion. As C_2 exists as a bound C_2Xe complex in the Xe matrix, its spectroscopy is expected to differ from that of free C_2. In Ne, Ar, and Kr matrixes, the valence state transitions of C_2 are relatively unperturbed and comparable to the gas-phase case.[4,5] Indeed, experiments have shown that the Mulliken (D ← X) and Phillips (A ← X) absorptions are only absent in Xe matrix.[4,5] A commonly given explanation of these observations is based on the assumption that C_2Xe is a well-bound molecule and as such its electronic structure and energetics are different from that of free C_2. This assertion can be tested by comparison of the calculated transition dipoles of C_2Kr and C_2-Xe (Figure 8). For an r_e of 4 Å for C_2Kr and 3.2 Å for C_2Xe, the Mulliken transition dipole moments gain in intensity from 1.7 D (Kr) and 3.6 D (Xe). Thus, the calculations of transition dipole moments show that internal C_2 transitions should either remain constant or even gain intensity in the presence of Xe, in contradiction with the experimental observations, and thus altered energetics of the complex must be responsible for their absence.

By inspection of the C_2Xe potentials (Figure 7), a few explanations can be proposed for the missing Mulliken band. As seen in Figures 6 and 7, the electronic states are strongly affected by the approaching Xe atom at distances of <3.5 Å, which corresponds to the ground-state minimum energy geometry. As r_e of C_2Xe in the ground state is shortened by over ∼0.7 Å from that of C_2Ar and C_2Kr, a vertical D ← X absorption in Xe places the excited-state wave packet on the steep repulsive wall of the D potential. This will create an absorption with larger natural lifetime broadening. Additionally, a nonadiabatic transition may be possible to the C state because of the presence of significant spin−orbit coupling in Xe. Finally, it may appear as the weak absorption at 300 nm (Figure 4), which would still fall within the accuracy of the potentials. Alternatively, these may belong to the charge-transfer states ($C_2^-Xe^+$). Absence of the Phillips band can be attributed to very steep repulsive potential in the upper A state at $r_e \sim 3$ Å. Such interaction would result in serious broadening of the spectral lines. Another reason for its disappearance could be related to interaction of the triplet state manifold with the A state.

Evaluation of the pair potentials could also provide explanation for the currently unassigned set of bands located at 423 nm (Figure 4). Strong experimental support for assigning the

423 nm band to a C_2 containing species, rather than C_3, was given by its direct correlation to the C_2Xe IR absorption.[4] The C_3 species is known to have UV absorption at 423 nm ($A\ (^1\Pi_u) \leftarrow X\ (^1\Sigma_g^+)$). The C_2^- Herzberg−Lagerqvist B $(^2\Sigma_u^+) \leftarrow X\ (^2\Sigma_u^+)$ (2,0) band, also found in this region (434 nm in Ar and Kr), can be removed from consideration by degree of structure contained in the 423 nm band set.[36] Considering the MCSCF excited states (Figure 7), the 423 nm band is energetically accessible by the forbidden $B' \leftarrow X$ transition, which becomes allowed via a breakdown of the u/g symmetry of C_2. Should the C_2 dopant be symmetrically centered in the substitutional site cavity, parity selection rules would once again be enabled. This fact would provide additional confirmation that C_2 exists asymmetrically centered in the large cavity, that is, bound to a single Xe atom. One unique feature is that Xe is the only rare gas host in which the band has been reported. At C_2Xe distance of 3 Å, the transition dipole moment was calculated to be ∼3.5 D indicating a strongly allowed transition.

Conclusions

Experimentally, we have recorded the UV absorption of acetylene photofragments in Ar, Kr, and Xe matrixes. For the Kr matrix, a previously unreported set of bands in the 188−209 nm region was found to belong to the same absorber, and by comparison of the spectrum to that of Cl and CN doped Kr matrixes and by theoretical predictions, the band set has been assigned to the C_2Kr_n neutral to $C_2^-Kr_n^+$ charge-transfer transitions.[7,8]

Large differences in energetics and structure of the C_2Xe triatomic were found from use of single and multiple reference computational methods. The HF based single reference methods including DFT[5] and CCSD(T) returned large binding energies (>1 eV) and a nonlinear minimum energy structure. A large deviation of the T_1 diagnostic of the CCSD(T) method from the accepted limit was found for configurations of short C_2Xe separation and nonlinear geometries. This indicated significant multireference character in the system at those points and the necessity for use of a multireference method. By varying the angle of the impinging Xe atom with respect to the C_2 molecular axis, we found the BCCD(T) method calculated the linear geometry to be a minimum at r_e in contrast to CCSD(T).

The Mulliken ($D \leftarrow X$) transition dipoles calculated by the MCSCF method are larger for C_2Xe than C_2Kr. This is in contrast to experimental findings in which both absorptions are absent in Xe[4,5] and questions the hypothesis that attributes the absence of these C_2 valence transitions to the formation of a C_2/Xe complex. Alternative explanations are proposed on the basis of evaluation of the excited-state potentials. Additionally, the band set found at ∼423 nm energetically match the $B' \leftarrow X$ transition.

References and Notes

(1) Apkarian, V. A.; Schwentner, N. *Chem. Rev.* **1999**, *99*, 1481.
(2) Jacox, M. E. *J. Phys. Chem. Ref. Data Suppl.* **2003**, *32*, 1.
(3) See, e.g.: Tanskanen, H.; Khriachtchev, L.; Kiljunen, H.; Räsänen, M. *J. Am. Chem. Soc.* **2003**, *125*, 16361, and references therein.
(4) Maier, G.; Lautz, C. *Eur. J. Org. Chem.* **1998**, 769.
(5) Frankowski, M.; Smith-Gicklhorn, A. M.; Bondybey, V. E. *Can. J. Chem.* **2004**, *82*, 837.
(6) Wang, H.; Szczepanski, J.; Vala, M. *Phys. Chem. Chem. Phys.* **2004**, *6*, 4090.
(7) Fiedler, S. L.; Vaskonen, K.; Ahokas, J.; Kunttu, H.; Eloranta, J.; Apkarian, V. A. *J. Chem. Phys.* **2002**, *117*, 8867.
(8) Fiedler, S.; Kunttu, H.; Eloranta, J. *Chem. Phys.* **2004**, *307*, 91.
(9) Breidung, J.; Thiel, W. *J. Mol. Spectrosc.* **2002**, *216*, 424.
(10) Milligan, D. E.; Jacox, M. E.; Abouf-Marguin, L. *J. Chem. Phys.* **1967**, *46*, 4562.
(11) Knowles, P. J.; Werner, H.-J. *Theor. Chim. Acta* **1992**, *84*, 95.
(12) Knowles, P. J.; Hampel, C.; Werner, H.-J. *J. Chem. Phys.* **1993**, *99*, 5219.
(13) Dunning, T. H., Jr. *J. Chem. Phys.* **1989**, *90*, 1007.
(14) Peterson, K. A.; Figgen, D.; Goll, E.; Stoll, H.; Dolg, M. *J. Chem. Phys.* **2003**, *119*, 1113.
(15) Müller, T.; Dallos, M.; Lischka, H.; Dubrovay, Z.; Szalay, P. *Theor. Chem. Acc.* **2001**, *105*, 227.
(16) Boys S. F.; Bernardi, F. *Mol. Phys.* **1970**, *19*, 553.
(17) Werner, H.-J.; Knowles, P. J. Amos, R. D.; Bernhardsson, A.; Berning, A.; Celani, P.; Cooper, D. L.; Deegan, M. J. O.; Dobbyn, A. J.; Eckert, F.; Hampel, C.; Hetzer, G.; Knowles, P. J.; Korona, T., Lindh, R.; Lloyd, A. W.; McNicholas, S. J.; Manby, F. R.; Meyer, W.; Mura, M. E.; Nicklass, A.; Palmieri, P.; Pitzer, R.; Rauhut, G.; Schütz, M.; Schumann, U.; Stoll, H.; Stone, A. J.; Tarroni, R.; Thorsteinsson, T.; Werner, H.-J. *MOLPRO*, version 2002.6; a package of ab initio programs.
(18) Feldman, V. I.; Sukhov, F. F.; Orlov, A. Y.; Tyulpina, I. V. *J. Am. Chem. Soc.* **2003**, *125*, 4698.
(19) Khriachtchev, L.; Tanskanen, H.; Lundell, J.; Pettersson, M.; Kijunen, H.; Räsänen, M. *J. Am. Chem. Soc.* **2003**, *125*, 4696.
(20) Plíva, J. *J. Mol. Spectrosc.* **1972**, *44*, 145.
(21) McDonald, S. A.; Johnson, G. L.; Keelan, B. W.; Andrews, L. *J. Am. Chem. Soc.* **1980**, *102*, 2892.
(22) Khriachtchev, L.; Tanskanen, H.; Cohen, A.; Gerber, R. B.; Lundell, J.; Pettersson, M.; Kiljunen, H.; Räsänen, M. *J. Am. Chem. Soc.* **2003**, *125*, 6876.
(23) Herman, M.; Campargue, A.; El Idrissi, M. I.; Van der Auwera, J. *J. Phys. Chem. Ref. Data* **2003**, *32*, 921.
(24) Bagdanskis, N. I.; Bulanin, M. O.; Fadeev, Yu. V. *Opt. Spektrosk.* **1970**, *29*, 687.
(25) Bryant, G. W.; Eggers, D. F.; Watts, R. O. *J. Chem. Soc, Faraday Trans. 2* **1988**, *84*, 1443.
(26) Kanamori, H.; Seki, K.; Hirota, E. *J. Chem. Phys.* **1987**, *87*, 73.
(27) Forney, D.; Jacox, M. E.; Thompson, W. E. *J. Mol. Spectrosc.* **1992**, *153*, 680.
(28) Andrews, L.; Kushto, G. P.; Zhou, M.; Wilson, S. P.; Souter, P. F. *J. Chem. Phys.* **1999**, *110*, 4457.
(29) Eloranta, J.; Kunttu, H. *J. Chem. Phys.* **2000**, *113*, 7446.
(30) Sato, H. *Chem. Rev.* **2001**, *101*, 2702.
(31) Creuzburg, M.; Koch, F.; Wittl, F. *Chem. Phys. Lett.* **1989**, *156*, 387.
(32) Lee T. J.; Taylor, P. R. *Int. J. Quantum Chem.* **1989**, *S23*, 199.
(33) Watts, J. D.; Bartlett R. J. *Int. J. Quantum Chem. Symp.* **1995**, *28*, 195
(34) *CRC Handbook of Chemistry and Physics*, 84th ed; Lide, D. R., Ed; CRC Press: Boca Raton, FL, 2003.
(35) Patel, K.; Butler, P. R.; Ellis, A. M.; Wheeler, M. D. *J. Chem. Phys.* **2003**, *119*, 909.
(36) Herzberg, G.; Lagerqvist, A. *Can. J. Phys.* **1968**, *46*, 2363.